ARS ADVANCED ROBOTIC SYSTEMS INTERNATIONAL

The Improved SVM Multi Objects's Identification For the Uncalibrated Visual Servoing

Xiangjin Zeng, Xinhan Huang and Min Wang
Dept. of Control Science and Engineering, Huazhong Univerisity of Science & Technology ; P.R China
xjzeng21@sohu.com

Abstract: *For the assembly of multi micro objects in micromanipulation, the first task is to identify multi micro parts. We present an improved support vector machine algorithm, which employs invariant moments based edge extraction to obtain feature attribute and then presents a heuristic attribute reduction algorithm based on rough set's discernibility matrix to obtain attribute reduction, with using support vector machine to identify and classify the targets. The visual servoing is the second task. For avoiding the complicated calibration of intrinsic parameter of camera, We apply an improved broyden's method to estimate the image jacobian matrix online, which employs chebyshev polynomial to construct a cost function to approximate the optimization value, obtaining a fast convergence for online estimation. Last, a two DOF visual controller based fuzzy adaptive PD control law for micro-manipulation is presented. The experiments of micro-assembly of micro parts in microscopes confirm that the proposed methods are effective and feasible.*

Keywords: *Micro-assembly, Support vector machine, Multi parts identification, Broyden method, Visual servoing*

1. Introduction

Micro-robot has a wide range of applications in micro-electromechanical systems. In order to assemble multi micro objects under microscope, it is necessary that identifies firstly these objects. In pattern recognition field, Moment feature is one of the shape feature that be used in extensive application. Invariant moments are the statistical properties of image, meeting that the translation, reduction and rotation are invariance. Hu (Hu, 1962) has present firstly invariant moments to be use for regional shape recognition. For closed structure and not closed structure, because the moment feature can not calculate directly, it need construct firstly regional structure. Besides, because the moment involves in the calculation of all the pixels of intra-regional and border, it means that it can be more time-consuming. Therefore, we apply the edge extraction algorithm to process image firstly, and then calculate the edge image's invariant moments to obtain the feature attribute, which solves the problem discussion above.

After feature attribute extraction, the classification algorithm should be provided during the final target identification. The main classifier used at present can be divided into three categories: One is the method statistics-based and its representative is such as the bayes methods, KNN method, like centre vector and SVM (Emanuela B & et al, 2003), (Jose L R & et al, 2004), (Yi X C & James Z W, 2003), (Jing P & et al, 2003), (Andrew H S & Srinivas M, 2003), (Kaibo D & et al, 2002); One is the method rule-based and its representative is decision tree and rough sets; The last one is the method based on artificial neural network. Being SVM algorithm is a convex optimization problems, its local optimal solution must be global optimal solution, which is better than the others learning algorithms. Therefore, we employ SVM classification algorithm to classify the targets. However, the classic SVM algorithm is established on the basis of the quadratic planning. That is, it can not distinguish the attribute's importance from training sample set. In additional with, It is high time to solve for the large volume data classification and time series prediction, which must improve its real-time data processing and shorten the training time and reduce the occupied space of the training sample set.

For the problem discussion above, presents an improved support vector machine classification, which applies edge extraction's invariant moments to obtain object's feature attribute. In order to enhance operation effectiveness and improve classification performance, a feature attribute reduction algorithm based on rough set (Richard Jensen & Qiang Shen, 2007), (Yu chang rui & et al, 2006) has been developed, with the good result to distinguish training data set's importance.

Then, In order to meet the request of the high precise micro-manipulation task, robotic must employ the visual servoing method. The methods of visual servoing need calibrate precisely intrinsic parameter of camera. However, the system calibration is the complicated and difficult problem, especially for micro-manipulation

International Journal of Advanced Robotic Systems, Vol. 6, No. 1 (2009)
ISSN 1729-8806, pp. 59-66

based on microscope vision. So, we present the uncalibrated method to estimate image jacobian matrix online.

Many papers (Kang Q. S & et al, 2006), (Malik A. S. & Choi T. S, 2007), (Shen, Song D & et al, 2003) have been reported some researches about image jacobian matrix online estimation. Piepmeier (Piepmeier, 1999, 2004) presents a moving target tracking task based on the quasi-Newton optimization method. This approach is adaptive, but cannot guarantee the stability of the visual servoing. Malis's (Malis E, 2004) method can keep the parameter of vision servo controller constant, when intrinsic parameter of camera is changed. Su J. et al (Su J. & et al, 2004) presents a motion 3D object tracking method based on the uncalibrated global vision feedback. Unfortunately, the current estimation methods have problems such as estimation-lag, singularity, convergence and its speed. Especially in dynamic circumstances, these problems become more serious. To deal with those problems discussed above, we apply an broyden's method to estimate the image jacobian matrix. The method employs chebyshev polynomial to construct a cost function to approximate the optimization value, improving the converge of estimation.

To verify the effectiveness of the methods, using the estimated jacobian matrix, a PD visual controller is used to make features converge to desired values with satisfactory dynamic performance. The experiments of micro-assembly of micro parts in microscopes confirm that the proposed method is effective and feasible.

2. The multi objects identification

2.1. Invariant moments thorty

Image $(p+q)$ order moments: we presume that $f(i,j)$ represents the two-dimensional continuous function. Then, it's $(p+q)$ order moments can be written as (1).

$$M_{pq} = \int\int i^p j^q f(i,j) didj \quad (p,q = 0,1,2...) \tag{1}$$

In terms of image computation, we use generally the sum formula of $(p+q)$ order moments shown as (2).

$$M_{pq} = \sum_{i=1}^{M}\sum_{j=1}^{N} f(i,j) i^p j^q \quad (p,q = 0,1,2...) \tag{2}$$

Where p and q can choose all of the non-negative integer value, they create infinite sets of the moment. According to papulisi's theorem, the infinite sets can determine completely two-dimensional image $f(i,j)$.

In order to ensure location invariance of the shape feature, we must compute the image $(p+q)$ order center moment. That is, calculates the invariant moments using the center of object as the origin of the image. The center of object $(i^{'}, j^{'})$ can obtain from zero-order moment and first-order moment. The centre-moment formula can be shown as (3).

$$M_{pq} = \sum_{i=1}^{M}\sum_{j=1}^{N} f(i,j)(i-i^{'})^p (j-j^{'})^q \quad (p,q = 0,1,2...) \tag{3}$$

At present, most studies about the two-dimensional invariant moments focus on extracting the moment from the full image. This should increase the computation amount and can impact on the real-time of system. Therefore, we propose the invariant moments method based on edge extraction, which gets firstly the edge image and then achieve the invariant moments feature attribute. Obviously, it keeps the region feature of moment using the propose method. In addition, being the role of edge detection, the data that participate calculation have made a sharp decline, reducing greatly the computation amount.

The invariant moments is the function of the seven moments, meeting the invariance of the translation, rotation and scale. The calculation formula is shown in (4).

$$\begin{aligned}
&\Phi_1 = m_{20} + m_{02} \\
&\Phi_2 = (m_{20} - m_{02})^2 + 4m_{11} \\
&\Phi_3 = (m_{30} - 3m_{12})^2 + (3m_{21} - m_{03})^2 \\
&\Phi_4 = (m_{30} + m_{12})^2 + (m_{21} + m_{03})^2 \\
&\Phi_5 = (m_{30} - 3m_{12})^2 (m_{30} + m_{12})[(m_{30} + m_{12})^2 - 3(m_{21} + m_{03})^2] \\
&+(3m_{21} - m_{03})(m_{21} - m_{03}) * [3(m_{30} + m_{12})^2 - (m_{21} + m_{03})^2] \\
&\Phi_6 = (m_{20} - m_{02})[(m_{30} + m_{12})^2 - 3(m_{21} + m_{03})^2] + \\
&4m_{11}(m_{30} + m_{12})(m_{21} + m_{03}) \\
&\Phi_7 = (3m_{12} - m_{30})^2 (m_{30} + m_{12})[(m_{30} + m_{12})^2 - 3(m_{21} + m_{03})^2] \\
&-(m_{03} - 3m_{21}) * [3(m_{30} + m_{12})^2 - (m_{21} + m_{03})^2]
\end{aligned} \tag{4}$$

We uses both of the seven moments function for computing the micro-object feature. The fivth section will give the experiments in detail.

2.2. Improved support vector machine and target identify

1) Support Vector Machine: The basic idea of SVM is that applies a nonlinear mapping Φ to map the data of input space into a higher dimensional feature space, and then does the linear classification in this high-dimensional space.

Presumes that the sample set (x_i, y_i), $(i = 1,...,n)$, $x \in R_d$ can be separated linearly, where x is d dimensional feature vector and $y \in \{-1,1\}$ is the class label. The general form of judgement function in its linear space is $f(x) = w \bullet x + b$. Then, the classification hyperplane equation can be shown as (5).

$$w \bullet x + b = 0 \tag{5}$$

If class m and n can be separated linearly in the set, there exists (w, b) to meet formula as (6).

$$\begin{aligned}
w \bullet x_i + b > 0, (x_i \in m) \\
w \bullet x_i + b < 0, (x_i \in n)
\end{aligned} \tag{6}$$

Where w is weight vector and b is the classification threshold. According to (5), if w and b are zoom in or out

at the same time, the classification hyperplane in (5) will keep invariant . We presume that the all sample data meet $|f(x) \geq 1|$, and the samples that is closest classification hyperplane meet $|f(x) = 1|$, then, this classification gap is equivalent to $2/\|w\|$. So the classification gap is biggest when $\|w\|$ is minimum.

Although the support vector machine with a better classification performance, but it can only classify two types of samples, and the practical applications often require multiple categories of classification. As a result, SVM need to be extended to more categories of classification issues. For the identification of a number of small parts in micromanipulation, we applied the Taiwan scholar Liu presented method based on the "one-to-many" method of fuzzy support vector machine for multi-target classification.

2) Improved Support Vector Machine: For the completion of the sample training, it is a usually method that all the feature attribute values after normalization have been used for modeling, which will increase inevitably the computation amount and may lead to misjudge the classification system being some unnecessary feature attributes. Therefore, bringing a judgement method to distinguish the attribute importance may be necessary for us. So we employ rough set theory to complete the judgement for samples attribute's importance. Then, we carry out SVM forecast classification based the reduction attributes.

Now, we introduce rough set theory. The decision-making system is $S = (U, A, V, f)$, where U is the domain with a non-null limited set and $A = C \cup D$. C, D represents conditions and decision-making attributes set respectively. V is the range set of attributes ($V = \bigcup_{a \in A} V_a$), V_a is the range of attribute a. f is information function ($f : UXA \to V$). If exists $f(x,a) \in V_a$ under $\forall x \in U \quad a \in A$ and $\forall B \subseteq A$ is a subset of the conditions attributes set, we call that $Ind(B)$ is S's un-distinguish relationship. Formula $Ind(B) = \{(x,y) \in UXU \mid \forall a \in B, f(x,a) = f(y,a)\}$ represents that x and y is indivisible under subset B. Given $X \subseteq U$, $B(x_i)$ is the equivalent category including x_i in term of the equivalent relationship $Ind(B)$. We can define the next approximate set $\underline{B(X)}$ and the last approximate set $\overline{B(X)}$ of subset X as follows:

$$\underline{B(X)} = \{x_i \in U \mid B(x_i) \subseteq X\}$$

$$\overline{B(X)} = \{x_i \in U \mid B(x_i) \bigcap X \neq \phi\}$$

If there is $\overline{B(X)}$ - $\underline{B(X)} = \phi$, the set X is able to define set based on B. Otherwise, call X is the rough set based on B. The positive domain of X based on B are the objects set that can be determined to belong to X based knowledge B. Namely, $POS_B(X) = \underline{B(X)}$. The dependence of decision-making attributes D and conditions attributes C can be defined as follows.

$$\gamma(C, D) = card(POS_C(D)) / card(U)$$

Where $card(X)$ is the base number of the set X.

The attributes reduction of rough set is that the redundant attributes have been deleted but there is not loss information. The formula $R = \{R \quad R \subseteq C, \quad \gamma(R,D) = \gamma(C,D)\}$ is the reduction attributes set. Therefore, we can use equation attributes dependence as conditions for terminating iterative computing.

In order to complete the attribute reduction, we present a heuristic attribute reduction algorithm based-on rough set's discernibility matrix, which applies the frequency that attributes occurs in matrix as the heuristic rules and then obtains the minimum attributes's relative reduction . The discernibility matrix was introduced by Skowron and has been defined as (7):

$$(c_{ij}) = \begin{cases} a \in A : r(x_i) \neq r(x_j) & D(x_i) \neq D(x_j) \\ \varnothing & D(x_i) = D(x_j) \\ -1 & \forall r, \exists r(x_i) = r(x_j) \quad D(x_i) \neq D(x_j) \end{cases} \tag{7}$$

According to formula (7), The value of elements is the different attributes combination when the attributes for the decision-making are different and the attributes for the conditions are different. The value of elements is null when the attributes for the decision-making are same. The value of elements is -1 when the attributes for the decision-making are same and the attributes for the conditions are different.

If p (a) is the attribute importance formula of attribute a, we can propose the formula as (8) according to the frequency that attribute occurs:

$$p(a) = \gamma \frac{1}{\left|U^2\right|} \sum_{a \in c_{ij}} \frac{1}{\left|c_{ij}\right|} \tag{8}$$

Where γ is the general parameter and c_{ij} are the elements of the discernibility matrix. Obviously, the greater the frequency that attribute occurs, the greater its importance. Therefore, we can compute the importance of attributes and eliminate the attributes that it's importance is the smallest using the heuristic rules in formula (8). And then, we can obtain the relative reduction attributes.

Now, we give the heuristics attribute reduction algorithm based-on rough set's discernibility matrix.

Input: the decision-making table $(U, A \cup D, V, f)$

Output: the relative attribute reduction

Algorithm steps:

1. computes the identification discernibility matrix M.
2. determines the core attributes and find the attributes combination that the core attributes is not included.
3. obtains conjunctive normal form $P = \wedge(\vee c_{ij} : (i = 1,2,3...s; j = 1,2,3...m))$ of the attributes combination by step (2), where c_{ij} are elements of each

attribute combination. And then converts the conjunctive normal form to disjunctive normal form.
4. determines the importance of attribute according to formula (8).
5. computes the smallest importance of attributes by steps (4) and then eliminate the less importance attribute to obtain the attributes reduction.

After the attribute has been reduced, the samples feature attributes will send to SVM for establishing model. Support vector machines using Gaussian kernel function, and Gaussian kernel function showed a good performance in practical applications of learning. Finally, we can finish the classification of the final prediction data.

3. Online estiamtion image Jacobian martrix

3.1. Image Jacobian

The image jacobian matrix J_q is defined as

$$\dot{f} = J_q(q)\dot{q} \tag{9}$$

Where

$$J_q(q) = \left[\frac{\partial f}{\partial q}\right] = \begin{bmatrix} \frac{\partial f_1(q)}{\partial q_1} & \cdots & \frac{\partial f_1(q)}{\partial q_m} \\ \cdots & & \cdots \\ \frac{\partial f_n(q)}{\partial q_1} & \cdots & \frac{\partial f_n(q)}{\partial q_m} \end{bmatrix} \tag{10}$$

$q = [q1, q2 \ldots qm]^R$ represents the coordinates of robot end-effector in the task space. $f = [f1, f2 \ldots fn]^T$ is corresponding position in image feature.

3.2. Image Jacobian matrix estimation based on broyden method

The image jacobian matrix can be calculated by calibrating the inner and outer parameter of robotic system & sensor system. However, it is impossible to obtain precise system parameter under a dynamic or uncertainty environment. Considering those, we employ broyden's method to estimate the image jacobian matrix.

The broyden method that solves the nonlinear equation can be shown in (11):

$$A_{k+1} = A_k + \frac{(y^{(k)} - A_k s^{(k)}) s^{(k)^T}}{\left\| s^{(k)} \right\|_2^2} \quad \text{k=0, 1…} \tag{11}$$

Now, we apply the broyden method to construct estimation model of image jacobian matrix. According to equation (1), if the feature error of two images represents as

$$e\ (q) = f^d - f^c \tag{12}$$

Where f^d is the feature of the expectation image and f^c is the feature of the current image, The taylor series expansion of e_f is shown as

$$e_f(q) = e_f(q_m) + \frac{\partial e(q_m)}{\partial q}(q - q_m) + \ldots + R_n(x) \tag{13}$$

Where $R_n(x)$ is Lagrange remaining. We define $\overset{*}{J}_q(q_n)$ as the Nth image jacobian to be estimated,

$$\overset{*}{J}_q(q) = \frac{\partial e(q_n)}{\partial q} \tag{14}$$

Ignoring the high order term and Lagrange remaining $R_n(x)$, Equation (15) can be obtained from (13) and (14), which is shown as

$$e_f(q) = e_f(q_m) + \overset{*}{J}_q(q_n)(q - q_m) \tag{15}$$

So, if J's counterpoint is A, Δe's counterpoint is y and Δq's counterpoint is s, we can construct the image jacobian estimation model based broyden. The image jacobian estimation model based on broyden method is shown as (16).

$$\overset{*}{J}_q(q_{k+1}) = \overset{*}{J}_q(q_k) + \frac{(\Delta e - \overset{*}{J}_q(q_k)\Delta q)\Delta q^T}{\Delta q^T \Delta q} \tag{16}$$

The broyden algorithm estimates the optimization value by employing iterative computation. Therefore, it need the end condition of iterative computation, we employ chebyshev polynomial to construct the cost function to approximate the optimization value.

3.3. The cost function based on chebyshev polynomail

Provided that

$$N_K(q) = e_f(q_k) + \overset{*}{J}_q(q)(q - q_k) \tag{17}$$

If $N_k(q) \in c[-1,1]$, for chebyshev polynomial serial $\{T_n, n = 0, 1, \ldots\}$ with weight $\rho(x) = (1 - x^2)^{-\frac{1}{2}}$, it's optimization square approximation polynomial can be shown as

$$s^*_n(x) = \frac{a_0}{2} + \sum_{i=1}^{n} a_i T_i(x) \tag{18}$$

where

$$a_i = \frac{2}{\pi}\int_{-1}^{1} \frac{N_k(x)T_i(x)}{\sqrt{1-x^2}}dx \qquad i = 0,1 \ldots n \tag{19}$$

Then

$$N(q) = \lim_{n\to\infty}\left(\frac{a_0}{2} + \sum_{i=1}^{n} a_i T_i(q)\right) \tag{20}$$

Usually, $N_k(q) \in c[a,b]$ we must convert $c[a,b]$ into $c[-1,1]$, The equation (21) can finish the convert.

$$t = \frac{b-a}{2}x + \frac{b+a}{2} \tag{21}$$

if we use part sum s^*_n as N(q)'s approximation, under some conditions, there is a fast speed for $a_n --> 0$.

3.4. Comparison chebyshev polynomial approximation

Piepmeier (Piepmeier, 1999, 2004) provides RLS algorithm to approximate best value for minimum cost function. The cost function using RLS is shown as (22).

$$Min(k) = \sum_{i=1}^{n} \lambda^{k-i} \left\| N_k(q_{i-1}) - N_{i-1}(q_{i-1}) \right\|^2 \tag{22}$$

where λ is a rate of dependency for prior data. As shown in equation (14), in order to obtain some performance, the cost function using RLS algorithm depends on the data of the several past steps, it mean that the prior knowledge must be obtained for finishing the task.

Similarly, the cost function using chebyshev polynomial is shown as (23).

$$M(k) = \sum_{i=1}^{n} \left\| N_k(q_{i-1}) - N_{i-1}(q_{i-1}) \right\|^2 \tag{23}$$

Clearly, the cost function using chebyshev polynomial is independent of the prior data.

3.5. Jacobian estimator with improved broyden method

A broyden with chebyshev polynomial approximate algorithm estimator of image jacobian is developed. A graphical representation of the estimate process is shown in Fig.1. Firstly, The broyden estimator starts with initial endeffector position q^0 and precision ε. Then, Camera captures an image of endeffector for extracting corresponding image coordinate feature f^k, which provides the possibility for calculating $\overset{*}{J}(q^k)$ by formula $\overset{*}{J}(q^k) = [f'(q^k)]^{-1}$. Secondly, Camera captures an image of target to obtain expectative image coordinate feature f^{k+1}. With the obtained $\overset{*}{J}(q^k)$, the servoing control law can be deduced detail in section of the vision controller design. Finally, Program judges whether precision ε satisfies system requirement or not. If precision ε arrives the requirement, system will be ended, otherwise system will be executed repeat processing.

4. The vision controller design

In order to finish three-dimensional small object positioning task, in the actual operation, micro-manipulation tasks will be divided into horizontal direction (XY plane) movement and the vertical direction (Z axis) movement. The manipulator in the XY plane moves first, positioning small parts in the above, then does so in the Z-axis vertical movement, positioning small parts at the centre. Therefore, we apply two image jacobian matrixs, including horizontial view field of image jacobian matrix and vertical view field of image jacobian matrix, which can complete the positioning and tracking three-dimensional objects.

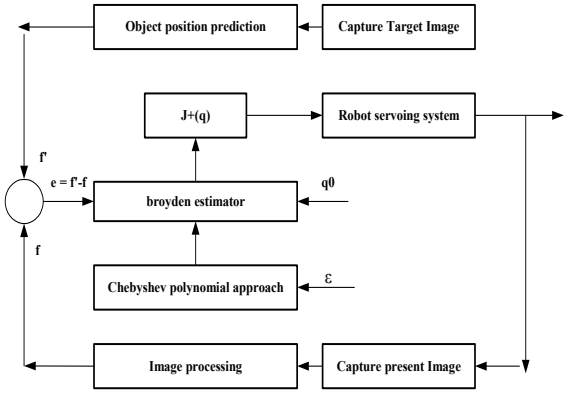

Fig. 1. A broyden with chebyshev polynomial approximation estimator of image jacobian

The change of robot movement $[dx, dy]^T$ and the change of image characteristics $[du, dv]^T$ can be wirte as (24):

$$\begin{bmatrix} dx \\ dy \end{bmatrix} = J \begin{bmatrix} du \\ dv \end{bmatrix} \tag{24}$$

According to the online estimtion image jacobian matrix J based on broyden method, sets the position of the error $e = f^d - f^c$, which f^d is the expectations of position of objects (small cylindrical parts, 600 um diameter) and f^c is the centre of endeffector. Then, the control law of PD controller u (k) is:

$$u(k) = K_p(\dot{J}^T\dot{J})^{-1}\dot{J}^T e(k) + K_d(\dot{J}^T\dot{J})^{-1}\dot{J}^T\frac{\Delta e(k)}{T_S} \tag{25}$$

Where T_s is the time interval, K_p is proportional gain and K_d is differential gain.

Since the microscope visual field is finite and controller is to avoid integral saturation, we design a two DOF visual controller based fuzzy adaptive PD control law for micro-manipulation.

The fuzzy adaptive PD controller applies error e and error change ec as its input. Then, we build a fuzzy rule table based practice experiences, which gives the counterpart relationship between Kp, Kd and error e, error change ec. So, we can revise online control system parameters. (26) shows the revised computation formula.

$$\begin{aligned} K_p &= K_p^* + \{e_i, ec_i\}_p \\ K_d &= K_d^* + \{e_i, ec_i\}_d \end{aligned} \tag{26}$$

5. Experiments

Micromanipulation robotic system includes 3D micro-move platform, micro-gripper driven by piezoelectricity, micro-adsorption hand driven by vacuum, microscope vision and so on. Micro-vision platform uses a two-way orthogonal optical vision, which includes the horizonal microscopes vision and the vertical microscopes vision.

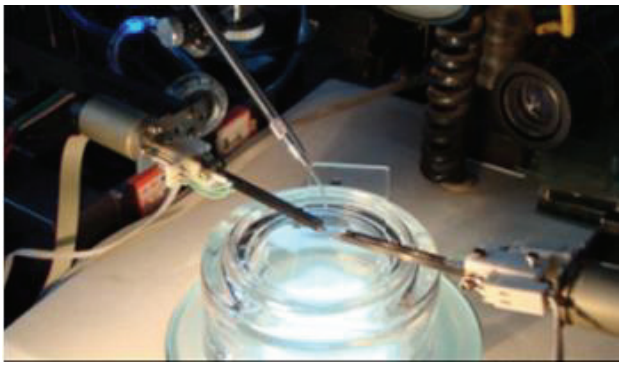

Fig. 2. The system construction of three hands cooperation micromanipulation stage

5.1. Feature extraction and data pretreat

The main task of classification is to identify and classify the manipulator (microgripper, vacuum suction) and operation targets (cylindrical metal part, glass ball), which can provide convenience for follow-up visual servo task. Fig.3 shows the original image of operation targets and manipulator in microscopic environment. Fig.4 is the image after edge extraction of operation targets and manipulator in microscopic environment.

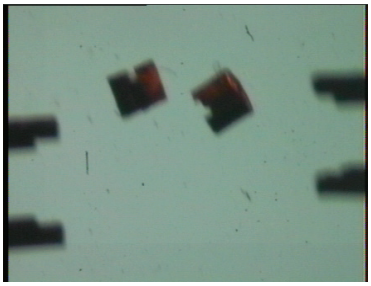

(a) Vertical view field of microscopic images

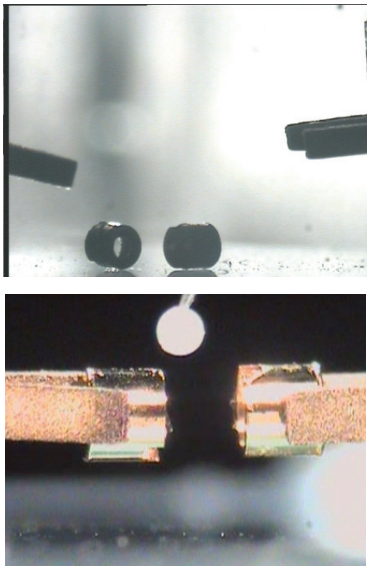

(b) Horizontal view field of microscopic images

Fig. 3. The original microscopic image of object and the endeffector in vertical (a) and horizontal (b) view fields

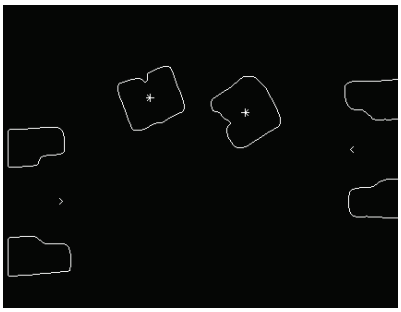

(a) Vertical view field of microscopic images

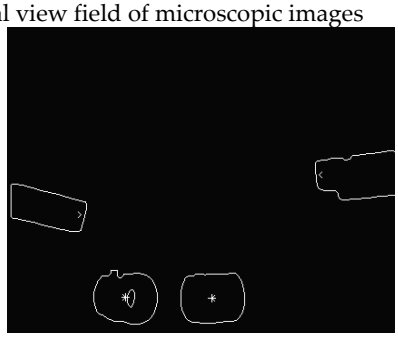

(b) Horizontal view field of microscopic images

Fig. 4. The object centre image and the end centre of the endeffector after processing in vertical (a) and horizontal (b) view fields

Table 1 gives the feature attribute's normalization value of four different objectives using invariant moments algorithm. We compute the feature attribute of objects in all directions and only list one of the feature attribute.

5.2. Result of identification and analysis

We compare firstly the data classification effectiveness on a number of micro objects using the traditional support vector machines algorithm and rough set + SVM, and the results are shown in table 2.

Category	F1	F 2	F 3	F4	F5	F6	F7
Cylindrical metal part	1.0000	-0.9910	0.9935	-0.1600	0.1076	1.0000	-0.5762
Glass Small Ball	1.0000	0.9900	-0.9946	0.1822	0.1178	0.9952	-0.5486
Micro Gripper	-0.9897	-0.7610	-1.0000	-1.0000	-0.9999	0.9554	-1.0000
Vacuum Suction	0.1673	0.9993	0.3131	0.9915	0.9857	-0.9577	0.9861

Table 1. The feature attribute's normalization value of different objects using invariant moments algorithm

	SVM		Rough set+SVM	
	Correction rate	Classification time	Correction rate	Classification time
Micro Object	93.45%	2108.24	95.89%	357.65

Table 2. The comparison results of using two classification methods

Times	Property	SVM classification accurateness	SVM+rough set classification accurateness
1	10	90%	95.10%
2	15	90.25%	96%
3	9	89%	92.87%
4	21	92.15%	97.08%
5	15	90.8%	92.33%
6	12	90%	93.5%
7	12	94%	95.22%
8	20	92.16%	97.4%

Table 3. The comparison results of classification accurateness using SVM and SVM+Rough set classification

According to table 2, the correction rate of classification based on the proposed SVM classification algorithm has been over 95 pre cent, being higher than the single SVM algorithm's correction rate. So, we can draw the conclusion that the attribute reduction improves the classification ability. Besides, compared with the single SVM algorithm's calculation time, It can be seen clearly from Table 2 that the calculation time of the proposed algorithm is less than about five times, meaning that the system becomes more effective.

Then, Table 3 provides the comparison results of classification accuracy using SVM classification and SVM+rough set classification with joining the other 25 feature attributes (gray, area, perimeter, texture, etc.). In table 3, The first column is times of data sets; second column is the number of conditions attributes after attribute reduction; third column is classification accuracy using the SVM; fourth column is classification accuracy using SVM and rough set algorithm. The number of conditions attributes of the final classification for entering to SVM is 14.25, less than 25 features attribute. Thus it simplifies the follow-up SVM forecast classification process.

5.3. Automatic position test

To accomplish micromanipulator positioning and girpping small parts, we must first obtain the centre of object and the centre of the end of endeffector. The centre of object and the end of endeffector can be accessed by a series of image processing (gray, de-noising and filter, canny operator, edge extraction, fuzzy c-means clustering). In Fig.5, the XY image plane coordinates of the center of the object is (147,99) and the centre of the end of the endeffector is (343,77).

Assuming that the initial parameters of PD controller Kp is 10 and Kd is 0, that is, only joined proportional control,

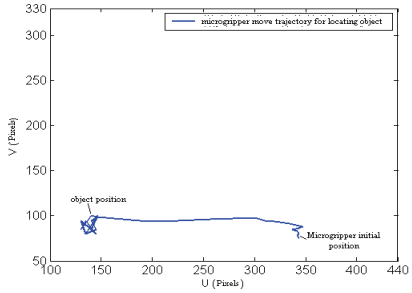

Fig. 5. The trajectories of micromanipulator approaching goal objects with only proportional control (XY plane)

control effect is shown in Fig. 5. We can see the implementation of automatic positioning objects to the target center, a greater oscillation and overshoot. When

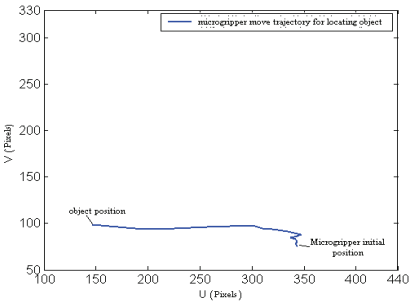

Fig. 6. The trajectories of micromanipulator approaching goal objects with proportional and differential control (XY plane)

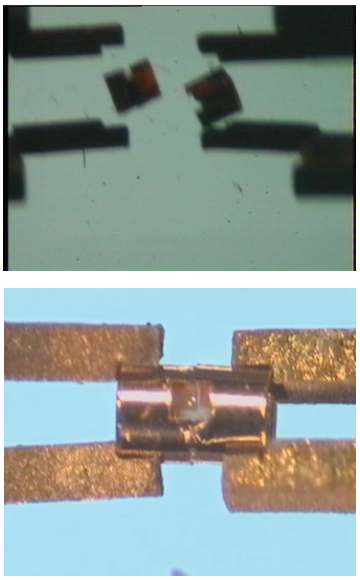

(a) Vertical view field of microscopic images

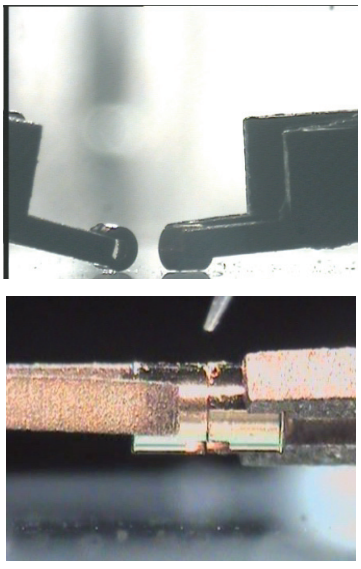

(b) Horizontal view field of microscopic images

Fig. 7. The image of endeffector automatically locating and gripping object in vertical (a) and horizontal (b) view fields

Kp is 10 and Kd is 1.5, which incorporates proportional and differential control, control result is shown in Fig.6. Differential joined inhibits apparently the system overshoot, and the system meets the rapid and smooth. Finally, the implementation of micro-manipulator positioning and automatic gripping operations is given, It can be obtained the satisfied implementation with the results to the system application requirements. Fig.7 is the image of the endeffector automatically locating object.

6. Conclusion

For the completion of three-dimensional micro-sized components assembly, an improved support vector machine algorithm is present, which be employed to identify multi micro objects. Then, We apply an improved broyden's method to estimate the image jacobian matrix on line, which employs chebyshev polynomial to construct a cost function to approximate the optimization value. Finally, design a PD controller to control micro-robot. In the microscopic visual environment, completes the visual servo task of micromanipulator positioning and automatic gripping small parts, the experimental results show that the algorithm is relatively satisfied with the effectiveness of implementation. The method that we presented not only ensures the existence of a local minimizer but also allows the convergence of the updated solution to the minimum. Howerver, it can get stuck on a saddle-point, in Newton's method, a saddle-point can be detected during modifications of the Hessian.

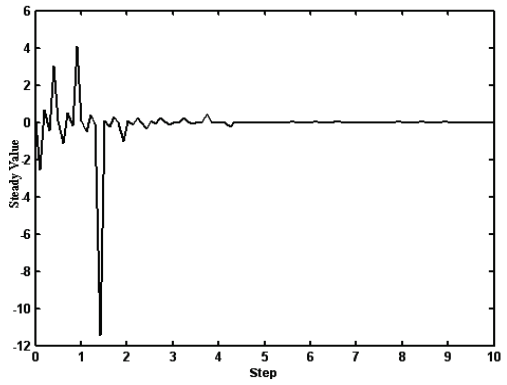

(a)

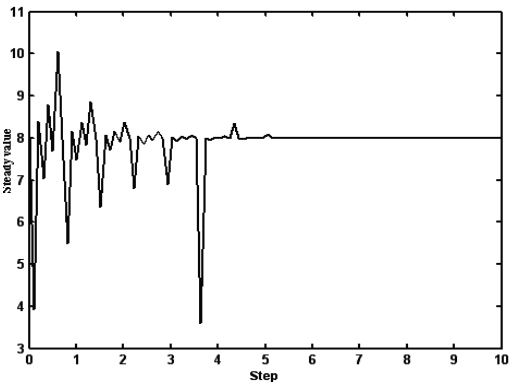

(b)

Fig. 8. Convergence speed of chebyshev algorithm (a) and Convergence speed of RLS (b)

7. References

Hu M K. (1962). Visual attribute recognition by moment invariants. IEEE Trans on Information Theory, vol. 8, pp. 179-187.

Emanuela B, Andrea B and Salvatore C. (2003). An innovative real time technique for buried object detection. IEEE Trans on Geoscience and Remote Sensing, vol.40, no.4, pp. 927-931.

Jose L R, Manel M and Mario D P. (2004). Support vector method for robot ARMA system identification. IEEE trans on signal processing, vol.52, no.1, pp. 155-164.

Yi X C & James Z W. (2003). Support vector learning for fuzzy rule based classification systems. IEEE trans on fuzzy system, vol.11, no.1, pp. 716-727.

Jing P, Douglas R H and Dai H K. (2003). LDA/SVM driven nearest neighbor classification. IEEE trans on neural networks, vol.14, no.4, pp. 940-942.

Andrew H S & Srinivas M. (2003). Identifying important features for intrusion detection using support vector machines and neural networks. Proceedings of the 2003 symposium on applications and internet.

Kaibo D, Keerthi S S and Aun N P. (2002). Evaluation of simple performance measures for tuning SVM hyperparameters. Neurocomputing, pp.1-19.

Richard Jensen & Qiang Shen. (2007). Fuzzy rough sets assisted attribute selection. IEEE transactions on fuzzy systems, vol.15, no.1, pp.73-89.

Kang Q. S., Hao T., Meng Z.D and Dai, X, Z. (2006). Pseudo inverse Estimation of Image jacobian Matrix in Uncalibration Visual Servoing. Proceedings of the 2006 IEEE International conference on Mechatronics and Automation ,pp.25-28.

Malik A. S. & Choi T. S. (2007). Consideration of illumination effects and optimization of window size for accurate calculation of depth map for 3D shape recovery. Pattern Recognition, vol.40, no.1,pp.154-170.

Shen, Song D., Liu Y. H and K Li. (2003). Asymptotic trajectory tracking of manipulators using uncalibrated visual feedback. IEEE/ASME Trans. on Mechatronics, vol.8, no.1, pp.87-98.

Piepmeier J. A., MacMurray G. V and Lipkin H. (1999). A Dynamic Quasi-Newton Method for Uncalibrated Visual Servoing. IEEE International Conference on Robotics and Automation , pp.1595-1600.

Piepmeier J. A. & MacMurray G. V. (2004). Lipkin H., Uncalibrated Dynamic Visual Servoing. IEEE Transactions on Robotics and Automation, vol.20, no.1, pp. 143-147.

Malis E. (2004). Visual servoing invariant to changes in camera-intrisic parameters. IEEE Trans. Robot. Autom, vol.20, no.1, pp.72–81.

Su J., Ma H., Qiu W and Xi Y. (2004). Task-independent robotic uncalibrated hand-eye coordination based on the extended state observer. IEEE Trans. on Systems, Man, and Cybernetics, vol.34, no.4, pp. 1917-1922.